Heliyon 10 (2024) e35123

Contents lists available at ScienceDirect

Heliyon

journal homepage: www.cell.com/heliyon

Research article

Determination of doxorubicin in plasma and tissues of mice by UPLC-MS/MS and its application to pharmacokinetic study

Zhilin Jin [a], Xue Xiao [b], Lili Gui [b], Qiao Lu [a,b,*], Jicai Zhang [a,c,**]

[a] Department of Laboratory Medicine, Taihe Hospital, Hubei University of Medicine, Shiyan, Hubei, 442000, China
[b] Hubei Key Laboratory of Wudang Local Chinese Medicine Research, Hubei University of Medicine, Shiyan, Hubei, 442000, China
[c] Hubei Key Laboratory of Embryonic Stem Cell Research, Hubei University of Medicine, Shiyan, Hubei, 442000, China

ARTICLE INFO

Keywords:
Doxorubicin
UPLC-MS/MS
Pharmacokinetics
Drug distribution

ABSTRACT

A rapid and sensitive ultra-high performance liquid chromatography-tandem mass spectrometry (UPLC-MS/MS) method was established for the simultaneous determination of doxorubicin (DOX) in mouse plasma and tissues, including the heart, liver, spleen, lung, kidney and tumor, and to investigate the pharmacokinetics and distribution in mice. In this study, daunorubicin (DNR) was used as an internal standard, and the mobile phase consisted of ammonium formate 2 mM containing 0.1 % formic acid (A) and acetonitrile (B), the chromatographic column was ACQUITY UPLC BEHTM C18 with a gradient elution at a flow rate of 0.2 mL/min. Electrospray ionization (ESI) in positive ion pattern was utilized for the ion separation of DOX, with the ions used for quantitative analysis being DOX *m/z* 544.28 → 397.10 and DNR *m/z* 528.35 → 321.08, respectively. The results showed that a good linear relationship in the calibration curve range of 1–800 ng/mL in mouse plasma and 1–2500 ng/g in tissues ($R^2 > 0.99$) with the limits of quantification of 1 ng/mL in plasma and tissues. The method exhibited good matrix effect and extraction recovery, with the intra-day and inter-day precision of plasma and tissue were less than 10.3 % and 15.4 %, and the relative error (RE) were both less than ±14.8 % and ±18.9 %, respectively. The stability results under different conditions were found to be accurate. It also revealed the distribution of DOX in various tissues of mice, with the concentration ranking as liver > heart > kidney > spleen > lung > tumor. This method was successfully used to the study for the pharmacokinetics in plasma and drug distribution in tissues of BALB/c mice.

1. Introduction

Doxorubicin (DOX), also known as adriamycin, its molecular structure formula is $C_{27}H_{29}NO_{11}$. It is an anthracycline anti-tumor antibiotic that eliminates tumor cells through the following two main mechanisms: (1) inhibiting the transcription and replication of DNA by intercalating two adjacent DNA base pairs, thereby inhibiting the activity of topoisomerase II; (2) generating a large number of oxygen free radicals (ROS), leading to damage in protein, lipid, membrane and DNA, ultimately inducing apoptosis in tumor cells [1–3]. At present, DOX is extensively utilized in the treatment of different clinical cancers including acute lymphoblastic leukemia, liver cancer, ovarian cancer, breast cancer, bladder cancer, lung cancer and gastric cancer [4–7]. However, DOX chemotherapy can

* Corresponding author. Department of Laboratory Medicine, Taihe Hospital, Hubei University of Medicine, Shiyan, Hubei, 442000, China.
** Corresponding author. Department of Laboratory Medicine, Taihe Hospital, Hubei University of Medicine, Shiyan, Hubei, 442000, China.
E-mail addresses: qiaolu@hbmu.edu.cn (Q. Lu), jicaizhang@taihehospital.com (J. Zhang).

https://doi.org/10.1016/j.heliyon.2024.e35123
Received 11 March 2024; Received in revised form 22 July 2024; Accepted 23 July 2024
Available online 26 July 2024

also result in some adverse reactions in the human body. The common side effects include acute myelosuppression (leukopenia and neutropenia, anemia and thrombocytopenia), neurotoxicity (numbness and pain in hands and feet), gastrointestinal reactions (nausea, vomiting, loss of appetite and even diarrhea), and subcutaneous tissue damage (rash, itching, pigmentation). In severe cases, it can lead to dose-dependent, mainly irreversible heart failure or arrhythmia [2,8–10]. Due to the above adverse reactions, the clinical application of DOX is constrained. In addition, because of its broad anticancer effects, DOX has been used on a large scale in clinical practice, resulting in drug resistance [11]. Therefore, when using DOX for chemotherapy treatment, it is particularly crucial to strictly control the dosage and monitor the process of DOX in patients including absorption, distribution, metabolism and excretion. This approach aims to maximize the bioavailability and therapeutic effects while reducing side effects.

Currently, the commonly employed quantitative methods for analyzing DOX in complex biological samples include liquid chromatography-ultraviolet (LC-UV), fluorescent spectrometry, fluorescence coupled capillary electrophoresis (CE-FL), and liquid chromatography-tandem mass spectrometry (LC-MS/MS) [12–15]. When compared with the LC-MS/MS method, ultraviolet and spectroscopy are simple and convenient, however, in practical application, these methods are not only time-consuming but also susceptible to interference from the endogenous substances in the samples or other co-detected analytes, leading to result deviations. In addition, the instrument exhibit poor sensitivity owing to the minimum detection limit is significantly lower than LC-MS/MS [16]. However, compared with the traditional LC-MS/MS, freshly ultra-high performance liquid chromatography-tandem mass spectrometry (UPLC-MS/MS) combines the highly selective separation ability of liquid chromatography (LC) with the sensitive detection ability of mass spectrometry (MS), which greatly improves the separation efficiency and rate, and is frequently used in the detection of the concentration of analytes which requires very low sensitivity [17]. Capillary electrophoresis is cost-effective, but its sensitivity and accuracy are lower than HPLC due to the small capillary diameter and the short optical path, and the sample components will be changed during the detection process, affecting the reproducibility of the separation results. The workflow of UPLC-MS/MS is the same as that of LC-MS/MS, involves that the LC columns with small particle size, such as hydrophilic column and C18 column, was used to separate the analytes from the complex biological components, following by further qualitative and quantitative analysis operating triple quadrupole MS on high pressure [18]. This method provides a higher resolution of chromatographic analysis, enhances the sensitivity and accuracy, and save the analysis time [19,20]. Up to now, it has emerged as one of the most accurate and reliable methods for detecting plasma drug concentration and has been widespread application in therapeutic drug monitoring (TDM), pharmacology, and toxicology in clinical biochemical diagnosis laboratories [21–23].

To date, numerous studies have reported on the metabolism and retention of DOX in mice, rats, or humans [24]. However, there is a paucity of research on the distribution of DOX in various tissues and solid tumors of mice. Due to the serious tissue damage resulting from a series of toxic reactions of DOX, particularly its potential for cardiotoxicity, nephrotoxicity, and hepatotoxicity, it is imperative to pay more attention to the utilization and distribution of drugs in tissues while closely monitoring tissue changes following drug administration [9,25,26]. Therefore, this study employed DNR as the internal standard and established a simple, rapid, and sensitive UPLC-MS/MS method for the determination of DOX in plasma, tissues and tumor in mice, with feasibility successfully verified. This approach holds great significance for clinical pharmacokinetic studies and drug concentration monitoring, providing valuable insights into the biodistribution and bioavailability of DOX in vivo, thereby offering theoretical guidance for clinical drug administration.

2. Materials and methods

2.1. Chemicals and reagents

Doxorubicin ($C_{27}H_{29}NO_{11}$, MW = 543.53) and daunorubicin (internal standard, IS, $C_{27}H_{29}NO_{10}$, MW = 527.52) were purchased from Yuanye Bio-Technology Co., Ltd. (Shanghai, China). They were in analytical level and used without further purification. Methanol, acetonitrile and ammonium formate were all of chromatographic grade and obtained from Sigma-Aldrich Co., Ltd. (Shanghai, China). Formic acid of chromatographic grade was sourced from Thermo Fisher Technology (Waltham, Massachusetts, U.S.A.). The water phase and all aqueous solutions were prepared by the Milli-Q ultrapure water system (Millipore, MA, U.S.A.) to a specific resistivity of 18.2 MΩ cm.

2.2. Cell culture and animals

The mouse breast cancer cell line 4T1 was provided by Procell Life Technology Co., Ltd. (Wuhan, China) and cultured in RPMI-1640 medium containing 10 % fetal bovine serum of Gibco (Grand Island, New York, U.S.A.) at 37 °C in a moist atmosphere containing 5 % CO_2. BALB/c mice (female, 4–6 weeks old) were provided by Beijing Weitong Lihua Experimental Animal Technology Co., Ltd. (license No. SCXK (E) 2022-0030). All mice had ad libitum access to water and food and underwent a fasting period of at least 12 h before the experiment. All animal experiments were conducted in accordance with the guidelines of the Ethics Review Committee for Animal Experimentation of Hubei University of Medicine (Ethics approval No. 2023-87).

When 4T1 cells reached the logarithmic growth phase, they were digested with trypsin (Gibco, Grand Island, New York, U.S.A.) and then centrifuged for 5 min at 1000 rpm. The upper medium was discarded and then PBS buffer (Gibco, Grand Island, New York, U.S.A.) was added. The 4T1 cells, with a density of 1×10^7 cells/mL, were injected into the left axilla of BALB/c mice, with approximately 100 μL cells were injected into each mouse. The subsequent experiments were conducted approximately 2 weeks after inoculation, when the tumor size had reached to 100–200 mm^3.

2.3. Mass spectrometry and liquid chromatography

The analytes DOX and DNR were analyzed using triple quadrupole tandem mass spectrometer (TSQ Quantiva, Thermo Fisher Scientific, Waltham, Massachusetts, U.S.A.). All runs were acquired and processed using Multi-Quant™ 3.0 software. The analytes were ionized by electrospray ionization (ESI) in positive ionization mode with multiple reaction monitoring mode (MRM). The ion source parameters for MS were as follows: ion injection voltage of 3500 V; sheath gas pressure of 35 psi; auxiliary gas pressure of 5 psi; sweep gas of 1 psi; ion delivery tube temperature of 325 °C; and vaporizer temperature of 350 °C. In the positive ionization mode, the radio frequency (RF) voltage for the analyte and internal standard was 58 V and 59 V, and the collision energy (CE) was 12 V and 25 V, respectively. The chromatographic instrument used was the UltiMate 3000 high-performance liquid chromatography (Thermo Fisher, U.S.A.). The chromatographic separations of analytes were carried out on an ACQUITY UPLC BEH™ C18 column (2.1 × 100 mm, 1.7 μm, Waters, Shanghai, China) using mobile phases of (A) ammonium formate 2 mM containing 0.1 % formic acid and (B) acetonitrile at a flow rate of 0.2 mL/min. The injection volume was 3 μL, and the column temperature was maintained at 30 °C. The mobile phases were used in a gradient elution method as following: 0–8.0 min, 10 % B; 8.0–10.0 min, 60 % B; 10.0–10.1 min, 60%–100 % B; 10.1–12.0 min, 100 % B; 12.0–12.1 min, 100%–10 % B; 12.1–13.0 min, 10 % B. The total analysis time was 13 min.

2.4. Standard sample preparation

2.4.1. Preparation of calibration standard solutions, quality control solutions and internal standard

The 1.00 mg of DOX and the internal standard DNR were accurately weighed and dissolved to prepare an original solution with a final concentration of 1 mg/mL using ultra-pure water. The original solution was further diluted with acetonitrile-water to prepare the working solution, Additionally, the original solution of DOX was diluted with 50 % acetonitrile-water (acetonitrile: water = 1:1) to prepared a standard working solution with concentrations of 2, 10, 20, 40, 80, 100, 200, 400, 1000, 1600 ng/mL. The concentrations of DOX quality control (QC) working solution were 1600, 160 and 16 ng/mL, respectively. The internal standard was diluted to 200 ng/mL using 50 % acetonitrile-water. The calibration standard curve and quality control of DOX were prepared using blank plasma or blank tissues. The concentration of plasma calibration curve was within the range of 1–1000 ng/mL, and the concentrations of the low, medium and high-quality control solutions (LQC, MQC, HQC) were 8, 80 and 800 ng/mL, respectively. The concentration range of calibration curve for each tissue was different, and the concentrations of LQC, MQC, HQC were 4, 80 and 800 ng/mL. All solutions were stored at −20 °C until analyzed.

2.4.2. Pretreatment of plasma and tissue samples

The protein precipitation method (PPT) was used for the pretreatment of mouse plasma and tissue samples. For tissue samples, homogenized was performed by fully homogenizing the samples in the Tissue Multi-channel Homogenizer (QIAGEN Kaijie TissueLyserII, Shanghai, China) after adding 1 mL of normal saline to 0.1 g of tissue. Firstly, the plasma or tissue homogenate samples (50 μL) were mixed with 50 μL of the same volume of internal standard solution (200 ng/mL) and 50 μL of 50 % acetonitrile-water, and then vortexed for 1 min. Subsequently, 225 μL acetonitrile was added to the solution and fully vortexed mixing for 2 min, with the entire process being carried out on ice. The supernatant was then transferred to a clean centrifuge tube by centrifugation for 15 min at 12,000 rpm at 4 °C. After filtering with a 0.22 μm membrane filter, the sample was transferred to 1.5 mL sample injection vials and stored at 4 °C until quantified and analyzed by LC-MS/MS.

2.5. Method validation

The study was validated in according with the International Conference on Harmonization guidelines for bioanalysis methods [27,28]. The assessment of exclusivity and specificity, matrix effect, recovery, linearity, precision and accuracy, as well as stability had been validated sequentially.

2.5.1. Exclusivity and specificity

The specificity of this method for the detection of analytes in plasma and tissues of mice needed to be verified. To verify the exclusivity and specificity of this method, the chromatograms of DOX and IS of the blank plasma or tissue samples of mice were compared with the lower limit of quantification (LLOQ) and the plasma or tissue samples of mice after 2 h of tail vein administration, so as to ensure that the endogenous substances in plasma or tissues did not interfere with the accurate detection of DOX and IS.

2.5.2. Matrix effect and extraction recovery

The low, medium and high concentration QC samples were prepared and treated by using three different methods: direct extraction samples (A), unextracted samples (B), and pure solution samples (C). The matrix effect was evaluated by comparing the average peak area between the unextracted (labeled QC and IS after extraction) and the corresponding blank matrix (water) [29–31]. The extraction recovery was determined by calculating the peak area ratio of extracted samples to unextracted samples. It was required that the extraction recovery and matrix effect RSD of DOX and IS in plasma or tissue should be less than or equal to 15 %.

$$\text{Matrix effect} = \text{Peak Area}_{(B)}/\text{Peak Area}_{(C)} \times 100\%, \quad (1)$$

$$\text{Recovery} = \text{Peak Area}_{(A)}/\text{Peak Area}_{(B)} \times 100\% \quad (2)$$

2.5.3. Linearity and calibration curve

In this study, $1/x^2$ weighted linear regression curve and the least square method were utilized to fit the curve. The ratio of DOX peak area to IS peak area was used as the ordinate of the plasma or tissue calibration curve, with the concentration of DOX as the abscissa. The standard curve of plasma or different tissues consisted of at least 5 data points, and the precision and accuracy achieved at each point within the linear range were required to meet the specified requirements.

2.5.4. Intra-and inter-day precision and accuracy

The precision test includes intra-day precision and inter-day precision. The precision and accuracy of the method were evaluated by comparing the concentrations of three different concentrations of QC (LQC, MQC, HQC) with the concentrations of DOX calculated by the standard curve on the same day. Each quality control level was prepared with plasma or tissue samples from 6 different sources, and the determination was repeated for 6 times. RSD (%) indicates precision and RE (%) indicates accuracy. The precision in plasma should be $\leq$ 15 %, and the acceptable range of accuracy should be within $\pm$15 %. For tissues, the acceptable range of precision and accuracy of different concentrations of QC should be within $\pm$20 %.

$$\text{Precision (RSD\%)} = (\text{SD}/\overline{x}) \times 100\%, \tag{3}$$

$$\text{Accuracy (RE\%)} = |\,\overline{x} - \text{QC}\,| \,/\, \text{QC} \times 100\% \tag{4}$$

SD: the standard deviations of the six results; $\overline{x}$: the mean value of the six results; QC: the quality controls

2.5.5. Stability

The stability of the method was evaluated by placing the quality control samples under the following three different conditions, including 4 h at room temperature (short-term stability), 12 h in an automatic injector (post-extraction stability), and repeated freezing and thawing for three times (freeze-thaw stability). Three plasma or tissue samples were determined for each quality control concentration (LQC, MQC, HQC). Comparing the theoretical concentration with the actual concentration, the final precision and accuracy of plasma and tissue were less than $\pm$15 % and $\pm$20 %, respectively, indicating that DOX could remain stable under different storage conditions of the experiment.

2.6. Application in pharmacokinetics and tissue distribution study

After the tumors of all mice had reached sufficient size, DOX at a concentration of 5 mg/kg was injected into the tail vein of BALB/c tumor mice. Blood samples, tissues and tumors were collected before (0 h) and at various time points after administration (25 min, 45 min, 1 h, 4 h, 6 h, 6 h, 8 h, 24 h, 48 h, 72 h). The blood samples were collected in heparin-containing centrifuge tubes and left at room temperature for more than 30 min. Subsequently, they were centrifuged for 15 min at 12,000 rpm at 4 °C, and the upper plasma was stored at −20 °C for pharmacokinetic study. The tissues (heart, liver, spleen, lung, kidney and tumor) were collected immediately after administration, and any residual blood on the surface was washed with normal saline. Finally, they were treated with liquid nitrogen and stored at −80 °C until the study of drug distribution.

3. Results and discussion

3.1. Optimization of mass spectrometry conditions

For MS conditions, we fine-tuned the electrospray ionization (ESI) scanning mode and associated source parameters. In the positive ion mode, both DOX and IS molecules were ionized to generate positively charged ions ($[M+H]^+$). The mass changes of DOX and internal standard DNR were *m/z* 544.28 → 397.10 and *m/z* 528.35 → 321.08, respectively. Compared with the negative ion mode, the positive ion mode exhibited higher sensitivity and selectivity to DOX and IS molecules. For the mixture of DOX and IS, the multiple reaction monitoring (MRM) scanning mode demonstrated stronger anti-interference ability and a lower detection limit than the selective reaction monitoring (SRM) scanning mode. At the same time, we manually optimized the ion source parameters of MS, as shown in Table 1. The mass spectra of the precursor ions and product ions obtained are shown in Fig. 1.

Table 1
The Mass-spectrometric ion-source parameters.

MS parameters	DOX/DNR
Spray Voltage (V)	3500
Sheath gas pressure (psi)	35
Aux gas pressure (psi)	5
Sweep gas (psi)	1
Ion transfer tube temp (°C)	325
Vaporizer temp (°C)	350

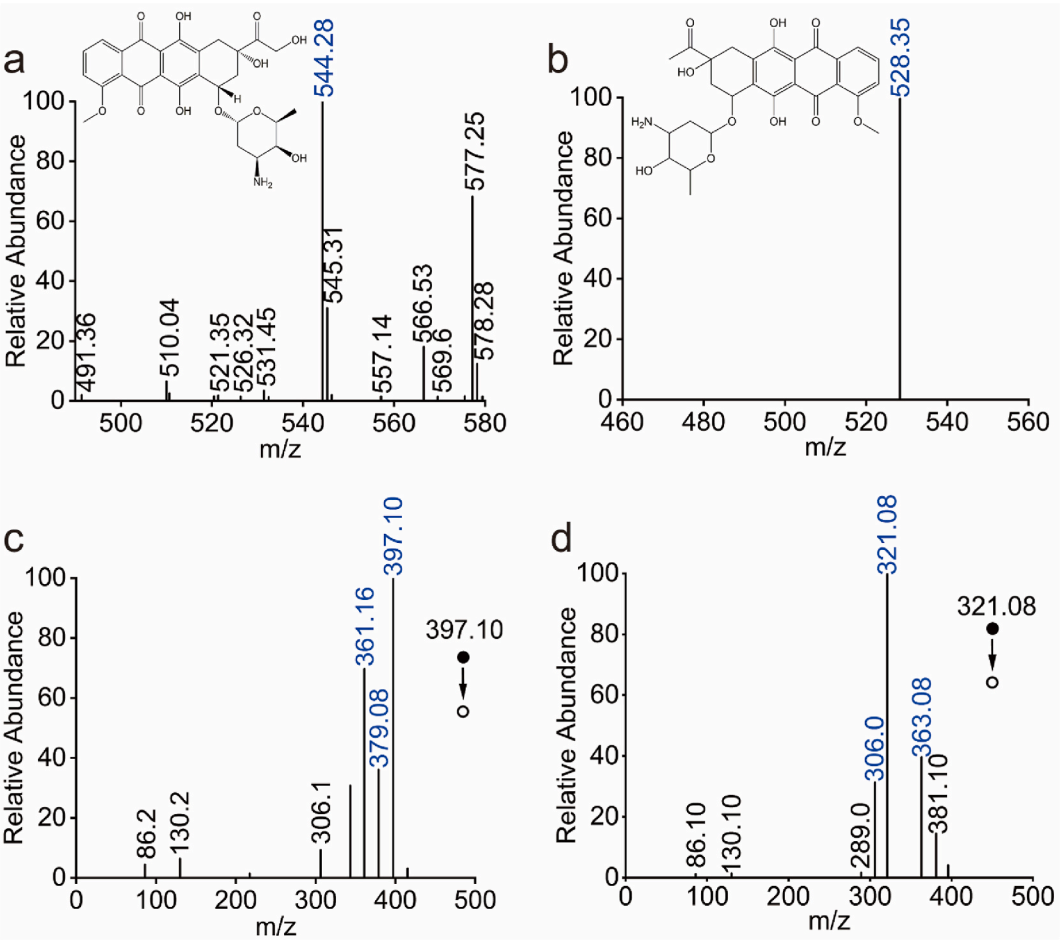

Fig. 1. The mass spectrograms in MRM mode: (a) The precursor ion of doxorubicin; (b) The precursor ion of daunorubicin; (c) The product ion of doxorubicin; (d) The product ion of daunorubicin.

3.2. Optimization of chromatographic conditions

For the optimization of chromatographic conditions, our main focus was on improving the separation ability and analytical effect of analytes through the optimization of chromatographic columns and flow conditions. We conducted experiments using various

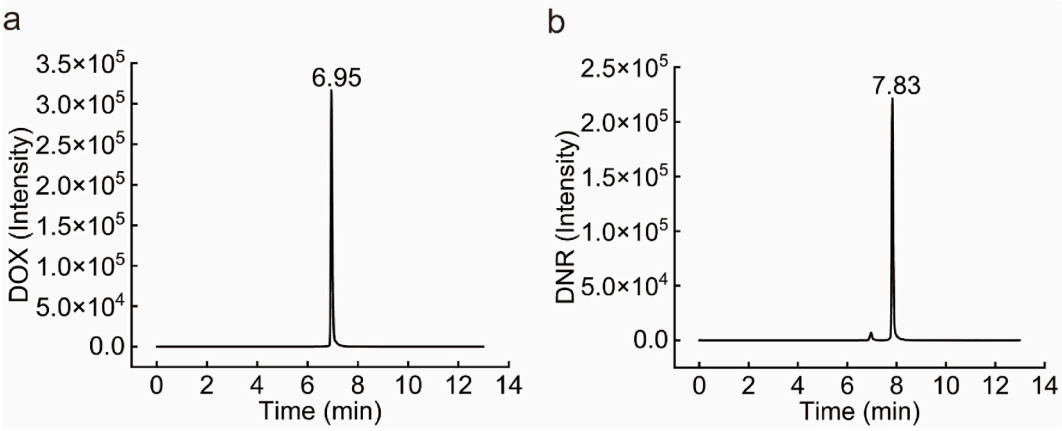

Fig. 2. Typical chromatogram: (a) doxorubicin; (b) daunorubicin (IS).

columns, mobile phase compositions, and proportions with different pH value. Using the ACQUITY UPLC BEH™ C18 column (2.1 × 100 mm, 1.7 μm) at a temperature of 30 °C with a gradient of ammonium formate 2 mM containing 0.1 % formic acid and acetonitrile as mobile phases, DOX and IS showed more symmetrical and higher peaks, resulting in a more intense response strength. Additionally, compared with isometric elution, gradient elution improved the chromatographic peak shape and shortens the separation time. The results showed that a mobile phase consisting of formic acid water containing ammonium formate (A) and acetonitrile (B) was used at a flow rate of 0.2 mL/min. The retention times of DOX and IS were 6.95 and 7.83 min, respectively, and the chromatogram is shown in Fig. 2.

3.3. Method validation

3.3.1. Exclusivity and specificity

The exclusivity and specificity of this method were determined by analyzing mouse plasma and homogenized tissue samples from

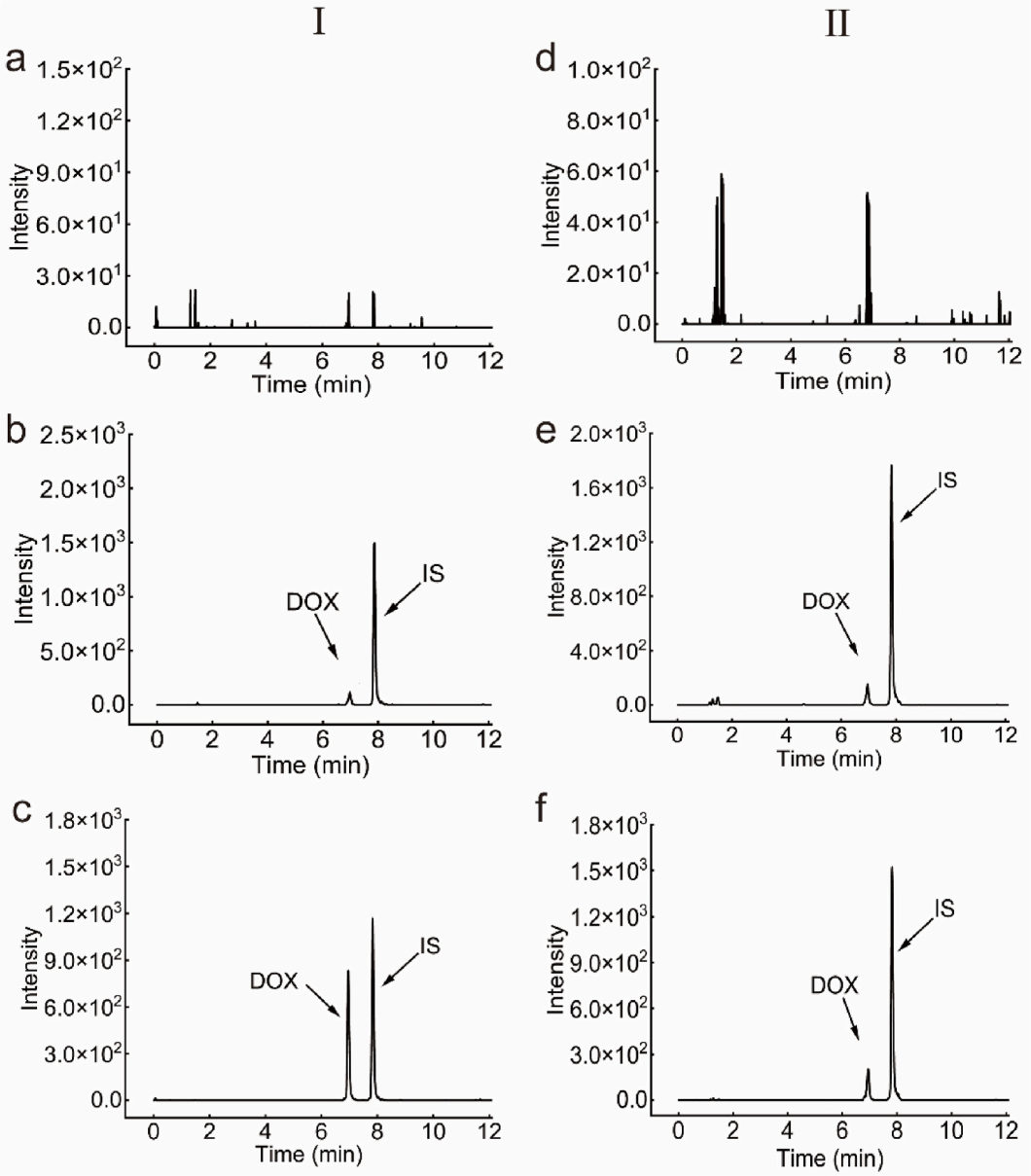

Fig. 3. Typical UPLC-MS/MS chromatograms of DOX and IS: (I) plasma; (II) kidney tissue; (a) blank plasma; (b) blank plasma after addition of DOX (LLOQ) and IS (100 ng/mL); (c) mouse plasma collected 2 h after intravenous injection of DOX (5 mg/kg); (d) blank kidney; (e) blank kidney after addition of DOX (LLOQ) and IS (100 ng/mL); (f) mouse kidney collected 2 h after intravenous injection of DOX (5 mg/kg).

six different sources. Take the kidney as an example of tissues, typical chromatograms of blank plasma and kidney samples are shown in Fig. 3. It was observed that there were only chromatographic peaks of DOX and internal standard DNR in the pictures, with their retention time (RT) demonstrating stability. This indicated that there was no obvious interference with the separation of the tested substances in the plasma or kidney homogenate of mice. Therefore, this method demonstrated strong exclusivity and specificity for the detection of DOX and IS.

3.3.2. Matrix effect and extraction recovery

In this study, we employed the protein precipitation method for the extraction of DOX from biological samples. This approach proved to be faster and simpler than both liquid-liquid extraction and solid-phase extraction, while also yielding superior extraction recovery. The matrix effect and extraction recovery of DOX and IS in plasma and kidney homogenate are detailed in Table 2. It was found that the optimal extraction recovery and minimum matrix effect were achieved when the samples were treated with 225 μL acetonitrile, following experimentation with various protein precipitants, including methanol and acetonitrile. The detection of six different sources of mouse plasma and tissues showed that the RSD of plasma matrix effect ranged from 2.6 % to 6.2 % with the extraction recovery of 3.4 %–9.0 %. The tissue matrix effect and recovery were found to be within the range of 12.2 %–15.5 % and 8.3 %–12.5 %, which aligns with the stipulations for biological analysis (basically $\leq$15 %). These results indicated that the method had no obvious matrix effect and satisfactory extraction recovery.

3.3.3. Linearity and calibration curve

The linear regression equation, linear range, and correlation coefficient (R^2) for DOX in plasma and tissues are shown in Table 3. The calibration curve demonstrated linearity within the following ranges: 1–800 ng/mL for plasma, 1–2500 ng/g for heart and spleen, 1–1000 ng/g for liver, kidney and tumor, and 1.25–1000 ng/g for lung. The correlation coefficient (R^2) for plasma was 0.9987, while the correlation coefficient for the tissues exceeded 0.99, which were in accordance with the regulations.

3.3.4. Intra-and inter-day precision and accuracy

The intra-day and inter-day precision and accuracy of plasma and kidney homogenate are shown in Table 4. In the quality control samples containing mouse plasma, all precision measurements were within 10.3 %, and the accuracy did not exceed 14.8 %, aligning with the stipulations outlined. For mouse tissue homogenate, the deviation remained below $\pm$20 % at all quality control concentration levels. Therefore, the findings were accurate and reliable, rendering this method suitable in the pharmacokinetics and drug distribution studies.

3.3.5. Stability

Table 5 displayed the stability of plasma and kidney homogenate under three distinct storage conditions. The results indicated that the precision in plasma meet the criteria, but the accuracy exceeded 15 % at the autosampler and room temperature at concentration of 8 ng/mL, which may be the cause of the DOX bit degradation. Likewise, precision and accuracy were consistently within the range of $\pm$20 % no matter what environment was placed in the organization. Hence, under varying experimental conditions, DOX remained largely stable, exerting minimal impact on the experimental results.

3.4. Application in pharmacokinetics and tissue distribution study

3.4.1. Pharmacokinetics study

We utilized UPLC-MS/MS method which had established to detect the plasma drug concentration of BALB/c mice injected with DOX (5 mg/kg) via the tail vein. The average blood concentration-time curve of mice is depicted in Fig. 4, and Origin software (OriginLab Corporation, version 9.1, Commonwealth of Massachusetts, U.S.A.) was utilized for curve analysis and visualization. The corresponding pharmacokinetic parameters are shown in Table 6, these parameters were calculated by DRUG AND STATISTICS software (DAS, version 2.0, Mathematical Pharmacology Professional Committee of China, Shanghai, China). The findings indicated that the peak concentration (C_{max}) in BALB/c mice was 183.0 $\pm$ 13.4 ng/mL, with a time to reach the maximum concentration (T_{max}) of 0.416 h. This demonstrated that DOX was fully absorbed within half an hour post-injection and subsequently circulated throughout

Table 2
Matrix effect and extraction recovery of DOX and IS in plasma and kidney tissue (n = 6).

Analytes	Concentration (ng/mL)	Extraction recovery (%)	RSD (%)	Matrix effects (%)	RSD (%)
Plasma					
DOX	8	89.1 ± 3.0	3.4	89.8 ± 2.3	2.6
	80	92.0 ± 3.8	4.1	106.8 ± 4.6	4.3
	800	94.7 ± 8.5	9.0	99.5 ± 6.2	6.2
DNR (IS)	100	98.8 ± 7.2	7.3	94.4 ± 3.8	4.1
Tissue					
DOX	4	94.1 ± 7.8	8.3	105.0 ± 12.8	12.2
	40	90.2 ± 11.3	12.5	94.2 ± 14.6	15.5
	800	75.5 ± 8.8	11.7	112.1 ± 17.2	15.4
DNR (IS)	100	111.2 ± 18.9	17.0	103.8 ± 17.0	16.4

Table 3
Linear relationship of DOX in plasma and tissue (n = 3).

Analytes	Standard curve	Linear range	R[b]
Plasma	Y = 0.01362 X + 0.01307	1–800	0.9987
Heart	Y = 0.01143 X + 0.00139	1–2500	0.9971
Liver	Y = 0.01354 X + 0.01375	1–1000	0.9973
Spleen	Y = 0.01605 X + 0.00365	1–2500	0.9982
Lung	Y = 0.01638 X + 0.00087	1.25–1000	0.9993
Kidney	Y = 0.01713 X + 0.00820	1–1000	0.9975
Tumor	Y = 0.01432 X + 0.00908	1–1000	0.9942

[a]The unit of drug concentration in plasma: ng/mL; The unit of drug concentration in tissues: ng/g.
[b]Y: the ratio of peaks; X: concentration.

Table 4
Inter-day precision and accuracy for DOX in plasma and kidney tissue (n = 6).

Concentration (ng/mL)	Intra-day			Inter-day		
	Measured concentration ± SD	Precision (RSD %)	Accuracy (RE %)	Measured concentration ± SD	Precision (RSD %)	Accuracy (RE %)
Plasma						
8	6.8 ± 0.2	3.5	−14.5	6.9 ± 0.3	4.8	−13.7
80	75.1 ± 2.5	3.4	−6.1	72.4 ± 2.4	3.3	−9.5
800	837.1 ± 85.9	10.3	4.6	811.8 ± 35.6	4.4	−14.8
Tissue						
4	3.2 ± 0.5	15.4	−18.9	3.4 ± 0.1	3.2	−15.0
40	34.9 ± 3.1	8.9	−12.7	34.5 ± 0.6	1.6	−13.7
800	718.1 ± 71.8	10.0	−10.2	721.8 ± 19.1	2.6	−9.8

Table 5
Stability of DOX under different storage conditions in plasma and kidney tissue (n = 3).

Conditions	Concentration (ng/mL or ng/g)	Measured concentration ± SD	Precision (RSD%)	Accuracy (RE%)
Plasma				
Autosampler stability (4 °C 12 h)	8	9.4 ± 0.5	5.8	18.1
	80	78.3 ± 0.7	0.8	−2.2
	800	835.5 ± 78.4	9.4	4.4
Room temperature stability (25 °C 4 h)	8	9.4 ± 0.4	3.8	17.1
	80	75.2 ± 6.9	9.2	−6.0
	800	785.8 ± 47.9	6.1	−1.8
Freeze thaw stability (−80 °C 3 times)	8	9.0 ± 1.2	13.4	12.6
	80	79.3 ± 2.3	2.9	−0.8
	800	811.4 ± 47.1	5.8	1.4
Tissue				
Autosampler stability (4 °C 12 h)	4	3.8 ± 0.5	12.4	−3.8
	40	33.0 ± 0.7	2.0	−17.5
	800	736.4 ± 36.8	5.0	−7.9
Room temperature stability (25 °C 4 h)	4	3.8 ± 0.4	11.0	−5.6
	40	32.1 ± 0.5	1.7	−19.8
	800	742.5 ± 54.4	7.3	−7.2
Freeze thaw stability (−80 °C 3 times)	4	3.8 ± 0.5	14.1	−3.9
	40	32.0 ± 0.8	2.4	−19.9
	800	677.4 ± 55.6	8.2	−15.3

the body. Similarly, the average retention time (MRT) of drug was 20.3 ± 4.2 h, indicating that DOX was almost exhausted approximately 24 h after a single intravenous administration in mice. The area under the concentration-time curve (AUC) revealed that the total amount of DOX entering the systemic circulation over the 72-h period was 2284.0 ± 248.7 mg/(L*h). Furthermore, the plasma half-life ($t_{1/2}$) of DOX was determined to be 22.3 ± 10.0 h, with a clearance rate of 0.002 L/kg per hour. The pharmacokinetic parameters may indicate the direction for the future clinical development of novel antineoplastic drugs.

3.4.2. Drug distribution in mice

In this study, we not only determined the DOX content in plasma, but also explored the metabolic process of drugs in various tissues and tumors of mice, culminating in the creation of a distribution map of DOX in various organs, illustrated in Fig. 5. It could be seen that the rapid dissemination of the drug throughout the mouse body, with the highest concentrations observed in the kidney, followed

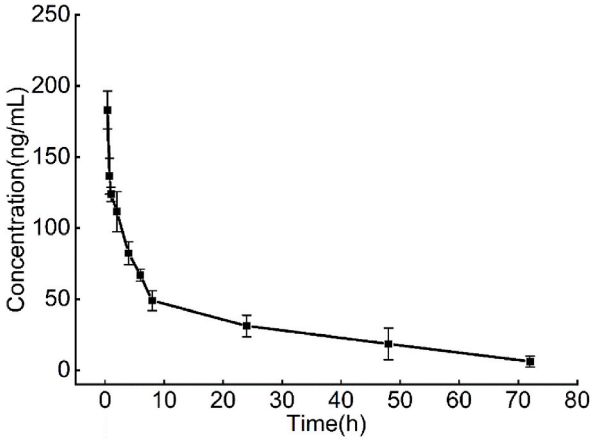

Fig. 4. The average plasma concentration-time curve of mice after intravenous injection of DOX (5 mg/kg) (mean ± SD, n = 3).

Table 6
Plasma concentration-time curve of DOX (n = 3, mean ± SD).

Parameter	Unit	DOX
C_{max}	mg/L	183.0 ± 13.4
T_{max}	h	0.416 ± 0.0
$AUC_{0\rightarrow t}$	mg/(L*h)	2284.0 ± 248.7
$AUC_{0\rightarrow \infty}$	mg/(L*h)	2512.7 ± 429.7
$t_{1/2}$	h	22.3 ± 10.0
CL	L/h/kg	0.002 ± 0.0
MRT	h	20.3 ± 4.2

C_{max}: Peak concentration; T_{max}: Peak time; AUC: Area under the concentration-time curve; $t_{1/2}$: Elimination half-life; CL: Clearance rate; MRT: Mean residence time.

by the liver, spleen, lung, heart, and tumor. The high concentration in the liver and kidney probably due to the predominant metabolism of antitumor drugs in these organs, while the notable presence in the mouse heart suggested potential cardiotoxicity. Numerous studies have consistently confirmed this result, the inevitable toxic effect of DOX on the heart, whether administered alone or in combination, and the degree of cardiac toxicity was different with different administration time, so heightened attention should be paid to this issue in clinical practice [32,33]. Therefore, the study was to provide a theoretical basis for clinicians to formulate different drug administration schemes, including considering reducing drug accumulation and side effects and ensuring a high degree of safety and effectiveness.

4. Conclusions

In summary, we had successfully developed and validated a simple, rapid and highly sensitive UPLC-MS/MS method for quantifying DOX in both plasma and various tissues, including heart, liver, spleen, lung, kidney, and tumor in mice, and verified the feasibility and accuracy of this method. This method exhibited good specificity, precision, and accuracy, with a remarkable linearity and R^2 exceeding 0.99. The LLOQ for DOX in plasma was 1 ng/mL, within a linear range of 1–800 ng/mL. Furthermore, we identified the LLOQ of DOX in heart, liver, spleen, lung, kidney, and tumor tissues to be 1, 1, 1, 1.25, 1, and 2 ng/mL, respectively. Furthermore, the sample processing method of protein precipitation is not only economical and convenient compared with other methods, but also enables the rapid extraction of the desired DOX from diverse samples. Subsequently, the extracted compound can be further separated and purified using a column for detection purposes. Following injection, the drug rapidly distributed in various organs of mice with the concentration in vivo ranking as kidney > liver > spleen > lung > heart > tumor. This study aimed to investigate the pharmacokinetics and tissue distribution of DOX in mice by analyzing its concentration in various biological samples, in order to provide valuable theoretical insights for the clinical administration of DOX as an antitumor drug in complex biological matrices.

Funding

This research was funded by the Natural Science Foundation of China (no. 22304050), Hubei Provincial Natural Science Foundation of China (no. 2023AFB271), The Open Project of Hubei Key Laboratory of Wudang Local Chinese Medicine Research (Hubei University of Medicine) (no. WDCM2023021) and Faculty Development Grants from Hubei University of Medicine (2022QDJZR007).

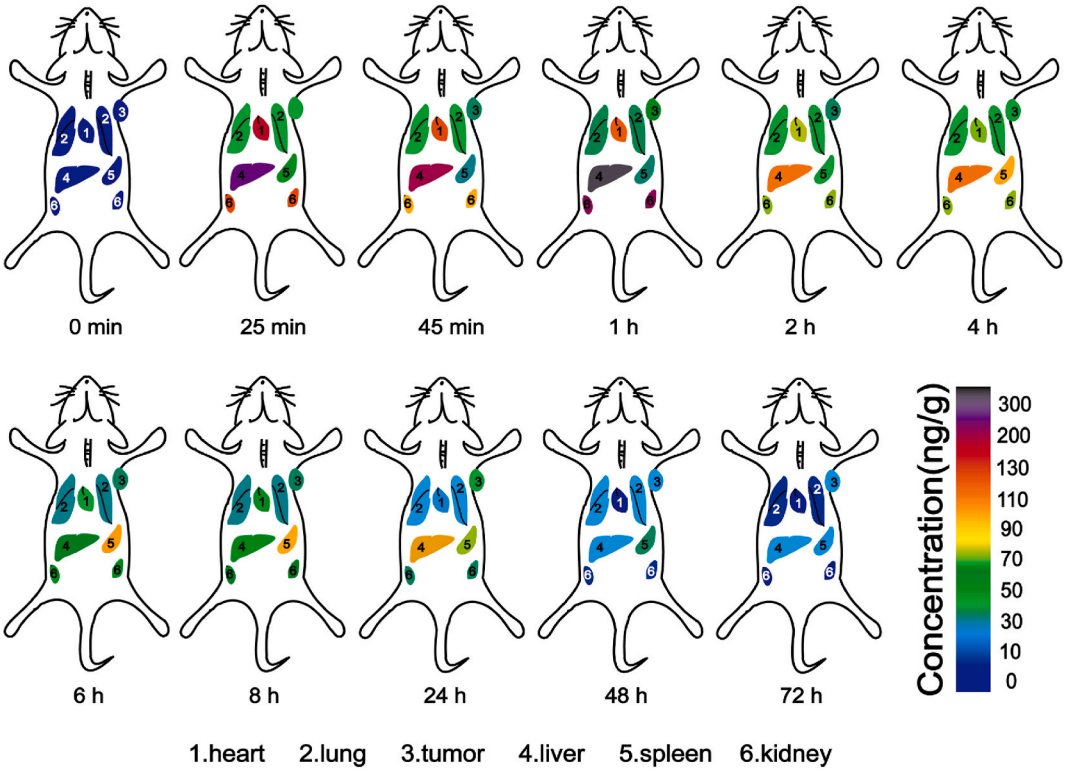

Fig. 5. Distribution of drugs in various tissues of mice after intravenous injection of DOX (5 mg/kg) (mean ± SD, n = 3).

Ethics statement

All animal experiments were conducted in accordance with the guidelines of the Ethics Review Committee for Animal Experimentation of Hubei University of Medicine (Ethics approval No. 2023-87).

Data availability statement

The data are available from the corresponding author on reasonable request. The data are not publicly available due to we have no public database and no link to archived datasets analyzed.

CRediT authorship contribution statement

Zhilin Jin: Writing – original draft, Investigation, Formal analysis, Conceptualization. **Xue Xiao:** Writing – review & editing, Investigation, Conceptualization. **Lili Gui:** Software, Data curation. **Qiao Lu:** Writing – review & editing, Supervision, Project administration. **Jicai Zhang:** Writing – review & editing, Supervision.

Declaration of competing interest

The authors declare that they have no known competing financial interests or personal relationships that could have appeared to influence the work reported in this paper.

Acknowledgments

This work was supported by the Biomedical Research Institute, Hubei University of Medicine. We are grateful for the instrumental and platform assistance provided by the laboratory.

Appendix A. Supplementary data

Supplementary data to this article can be found online at https://doi.org/10.1016/j.heliyon.2024.e35123.

References

[1] M. Kciuk, A. Gielecińska, S. Mujwar, D. Kołat, Ż. Kałuzińska-Kołat, I. Celik, R. Kontek, Doxorubicin—an agent with multiple mechanisms of anticancer activity, Cells 12 (2023) 659, https://doi.org/10.3390/cells12040659.

[2] S. Peter, S. Alven, R.B. Maseko, B.A. Aderibigbe, Doxorubicin-Based hybrid compounds as potential anticancer agents: a review, Molecules 27 (2022) 4478, https://doi.org/10.3390/molecules27144478.

[3] Y. Hu, P. Ma, L. Chen, J. Liu, Y. Shang, W. Jian, Multi-parameter cardiac magnetic resonance imaging detects anthracycline-induced cardiotoxicity in rabbits model, Heliyon 9 (2023) e21845, https://doi.org/10.1016/j.heliyon.2023.e21845.

[4] S. Sritharan, N. Sivalingam, A comprehensive review on time-tested anticancer drug doxorubicin, Life Sci. 278 (2021) 119527, https://doi.org/10.1016/j.lfs.2021.119527.

[5] Y.P. Fan, J.Z. Liao, Y.Q. Lu, D.A. Tian, F. Ye, P.X. Zhao, G.Y. Xiang, W.X. Tang, X.X. He, MiR-375 and doxorubicin Co-delivered by liposomes for combination therapy of hepatocellular carcinoma, Mol. Ther. Nucleic Acids 7 (2017) 181–189, https://doi.org/10.1016/j.omtn.2017.03.010.

[6] H. Zhao, J. Yu, R. Zhang, P. Chen, H. Jiang, W. Yu, Doxorubicin prodrug-based nanomedicines for the treatment of cancer, Eur. J. Med. Chem. 258 (2023) 115612, https://doi.org/10.1016/j.ejmech.2023.115612.

[7] Q. Lin, M. Zhang, Y. Kong, Z. Huang, Z. Zou, Z. Xiong, X. Xie, Z. Cao, W. Situ, J. Dong, S. Li, X. Zhu, Y. Huang, Risk score = LncRNAs associated with doxorubicin metabolism can be used as molecular markers for immune microenvironment and immunotherapy in non-small cell lung cancer, Heliyon 9 (2023) e13811, https://doi.org/10.1016/j.heliyon.2023.e13811.

[8] C. Carvalho, R.X. Santos, S. Cardoso, S. Correia, P.J. Oliveira, M.S. Santos, P.I. Moreira, Doxorubicin: the good, the bad and the ugly effect, Curr. Med. Chem. 16 (2009) 3267–3285, https://doi.org/10.2174/092986709788803312.

[9] L. Wu, L. Wang, Y. Du, Y. Zhang, J. Ren, Mitochondrial quality control mechanisms as therapeutic targets in doxorubicin-induced cardiotoxicity, Trends Pharmacol. Sci. 44 (2023) 34–49, https://doi.org/10.1016/j.tips.2022.10.003.

[10] P. Aleksandar, M.-Ć. Dragana, J. Nebojša, N. Biljana, S. Nataša, V. Branka, K.-V. Jelena, Wild edible onions — Allium flavum and Allium carinatum — successfully prevent adverse effects of chemotherapeutic drug doxorubicin, Biomed. Pharmacother. 109 (2019) 2482–2491, https://doi.org/10.1016/j.biopha.2018.11.106.

[11] M.H. Mukhtar, M.Z. El-Readi, M.E. Elzubier, S.H. Fatani, B. Refaat, U. Shaheen, E.B. Adam Khidir, H.H. Taha, S.Y. Eid, Cymbopogon citratus and citral overcome doxorubicin resistance in cancer cells via modulating the drug's metabolism, toxicity, and multidrug transporters, Molecules 28 (2023), https://doi.org/10.3390/molecules28083415.

[12] D. Kaushik, G. Bansal, Four new degradation products of doxorubicin: an application of forced degradation study and hyphenated chromatographic techniques, J. Pharm. Anal. 5 (2015) 285–295, https://doi.org/10.1016/j.jpha.2015.05.003.

[13] R. Belhoussine, H. Morjani, J.M. Millot, S. Sharonov, M. Manfait, Confocal scanning microspectrofluorometry reveals specific anthracyline accumulation in cytoplasmic organelles of multidrug-resistant cancer cells, J. Histochem. Cytochem. 46 (1998) 1369–1376, https://doi.org/10.1177/002215549804601205.

[14] T. Hong, R. Zheng, L. Qiu, S. Zhou, H. Chao, Y. Li, W. Rui, P. Cui, X. Ni, S. Tan, P. Jiang, J. Wang, Fluorescence coupled capillary electrophoresis as a strategy for tetrahedron DNA analysis, Talanta 228 (2021) 122225, https://doi.org/10.1016/j.talanta.2021.122225.

[15] P. Qi, P. Li, L. Qiao, H. Xue, Y. Ma, S. Wei, X. Yang, H. Zhang, Y. Zhang, Y. Wang, S. He, H. Quan, W. Zhang, Simultaneous quantification of pirarubicin, doxorubicin, cyclophosphamide, and vincristine in human plasma of patients with non-Hodgkin's lymphoma by LC–MS/MS method, J. Chromatogr. B 1224 (2023), https://doi.org/10.1016/j.jchromb.2023.123754.

[16] A. Suneetha, R.K. Raja, Comparison of LC-UV and LC–MS methods for simultaneous determination of teriflunomide, dimethyl fumarate and fampridine in human plasma: application to rat pharmacokinetic study, Biomed. Chromatogr. 30 (2016) 1371–1377, https://doi.org/10.1002/bmc.3694.

[17] F. Chen, Z. Yu, X. Wang, Development of a UPLC-MS/MS method for the determination of narciclasine and 7-deoxynarciclasine in mouse blood and its application in pharmacokinetics, J. Chromatogr. B 1180 (2021) 122899, https://doi.org/10.1016/j.jchromb.2021.122899.

[18] Y.-Y. Zhao, S.-P. Wu, S. Liu, Y. Zhang, R.-C. Lin, Ultra-performance liquid chromatography–mass spectrometry as a sensitive and powerful technology in lipidomic applications, Chem. Biol. Interact. 220 (2014) 181–192, https://doi.org/10.1016/j.cbi.2014.06.029.

[19] Z. Lei, D.V. Huhman, L.W. Sumner, Mass spectrometry strategies in metabolomics, J. Biol. Chem. 286 (2011) 25435–25442, https://doi.org/10.1074/jbc.R111.238691.

[20] S. Yılmazer Keskin, A. Avcı, H. Fajriana Febda Kurnia, Analyses of phytochemical compounds in the flowers and leaves of Spiraea japonica var. fortunei using UV-VIS, FTIR, and LC-MS techniques, Heliyon 10 (2024) e25496, https://doi.org/10.1016/j.heliyon.2024.e25496.

[21] N. Zheng, X. Wang, Y. Wang, G. Xu, H. Zhang, W. Dai, B. He, Q. Zhang, J. Ji, X. Wang, A sensitive liquid chromatography/electrospray tandem mass spectroscopy method for simultaneous quantification of a disulfide bond doxorubicin conjugation prodrug and activated doxorubicin: application to cellular pharmacokinetic and catabolism studies, J. Chromatogr. B 1065–1066 (2017) 96–103, https://doi.org/10.1016/j.jchromb.2017.09.035.

[22] R.F. Greaves, Recent advances in the clinical application of mass spectrometry, EJIFCC 27 (2016) 264–271.

[23] C. Seger, M. Shipkova, U. Christians, E.M. Billaud, P. Wang, D.W. Holt, M. Brunet, P.K. Kunicki, T. Pawinski, L.J. Langman, P. Marquet, M. Oellerich, E. Wieland, P. Wallemacq, Assuring the proper analytical performance of measurement procedures for immunosuppressive drug concentrations in clinical practice: recommendations of the International Association of Therapeutic Drug Monitoring and Clinical Toxicology Immunosuppressive Drug Scientific Committee, Ther. Drug Monit. 38 (2016) 170–189, https://doi.org/10.1097/FTD.0000000000000269.

[24] S.G. Espírito Santo, M.G. Monte, B.F. Polegato, L.F. Barbisan, G.R. Romualdo, Protective effects of omega-3 supplementation against doxorubicin-induced deleterious effects on the liver and kidneys of rats, Molecules 28 (2023), https://doi.org/10.3390/molecules28073004.

[25] M.A. Hussain, N.M. Abogresha, G. AbdelKader, R. Hassan, E.Z. Abdelaziz, S.M. Greish, F. Morroni, Antioxidant and anti-inflammatory effects of crocin ameliorate doxorubicin-induced nephrotoxicity in rats, Oxid. Med. Cell. Longevity 2021 (2021) 1–12, https://doi.org/10.1155/2021/8841726.

[26] T.O. Omobowale, A.A. Oyagbemi, U.E. Ajufo, O.A. Adejumobi, O.E. Ola-Davies, A.A. Adedapo, M.A. Yakubu, Ameliorative effect of gallic acid in doxorubicin-induced hepatotoxicity in Wistar rats through antioxidant defense system, J. Diet. Suppl. (15) (2017) 183–196, https://doi.org/10.1080/19390211.2017.1335822.

[27] A. Riezk, V. Vasikasin, R.C. Wilson, T.M. Rawson, J.G. McLeod, R. Dhillon, J. Duckers, A.E.G. Cass, A.H. Holmes, Triple quadrupole LC/MS method for the simultaneous quantitative measurement of cefiderocol and meropenem in serum, Anal. Methods 15 (2023) 746–751, https://doi.org/10.1039/d2ay01459a.

[28] International Council for Harmonisation of Technical Requirements for Pharmaceuticals for Human Use, ICH guideline Q2(R2) on validation of analytical procedures. Available online: https://www.ema.europa.eu/en/documents/scientific-guideline/ich-guideline-q2r2-validation-analytical-procedures-step-2b_en.pdf (accessed on March 24).

[29] M. Cortese, M.R. Gigliobianco, F. Magnoni, R. Censi, P. Di Martino, Compensate for or minimize matrix effects? Strategies for overcoming matrix effects in liquid chromatography-mass spectrometry technique: a tutorial review, Molecules 25 (2020) 3047, https://doi.org/10.3390/molecules25133047.

[30] A.D. Nicolò, M. Cantù, A. D'Avolio, Matrix effect management in liquid chromatography mass spectrometry: the internal standard normalized matrix effect, Bioanalysis 9 (2017) 1093–1105, https://doi.org/10.4155/bio-2017-0059.

[31] M.A.G.M. Kroon, H.W.M. van Laarhoven, E.L. Swart, E.M. Kemper, O. van Tellingen, A validated HPLC-MS/MS method for simultaneously analyzing curcumin, demethoxycurcumin, bisdemethoxycurcumin, tetra-hydrocurcumin and piperine in human plasma, urine or feces, Heliyon 9 (2023) e15540, https://doi.org/10.1016/j.heliyon.2023.e15540.

[32] S.Y. Saad, T.A.O. Najjar, M. Alashari, Cardiotoxicity of doxorubicin/paclitaxel combination in rats: effect of sequence and timing of administration, J. Biochem. Mol. Toxicol. 18 (2004) 78–86, https://doi.org/10.1002/jbt.20012.

[33] V. Valero, E. Perez, V. Dieras, Doxorubicin and taxane combination regimens for metastatic breast cancer: focus on cardiac effects, Semin. Oncol. 28 (2001) 15–23.